

# Improving Boundary Definition for 3D Ultrasound Quantification of Fetal Femur

M. Yaqub<sup>1,2</sup>, C. Ioannou<sup>3</sup>, A. Papageorghiou<sup>3</sup>, M. K. Javaid<sup>1</sup>, C. Cooper<sup>1</sup>, J. A. Noble<sup>2</sup>  
University of Oxford, departments of <sup>1</sup>NDORMS, <sup>2</sup>IBME, Engineering Science, <sup>3</sup>NDOG

---

**Abstract.** Although the quality of 3D and 4D ultrasound imaging continues to improve, it does not compare with CT or MRI in terms of anatomical definition. In the case of obstetrics however, ultrasound is the main imaging modality that can be used throughout pregnancy. For automatic volumetric quantification and diagnosis there is a clear need for novel methodology which maximizes the anatomical definition obtained from one or more ultrasound scans. In this paper, we propose an automatic 3D image fusion technique to combine multiple ultrasound images taken from different angles of the fetal femur. The material properties of the femoral tissues result in high attenuation of parts of the femur in a single scan. The main goal of this paper is to propose a method to enhance femur boundary definition and provide a complete anatomical image of the femur. Qualitative results on 8 patient scans show that the fused view is always ranked better or equal to the single view scans case. Quantitative analysis on the 8 datasets and a fetal phantom show a mean increase of contrast and signal to noise of about  $16\pm 18\%$  and  $8\pm 4\%$  respectively. In addition, comparisons of manual segmentation of two femurs in 4 single views and a fused view show that the percentage volume increase in the fused view is about 15%.

## 1 Introduction

Fetal Ultrasound (US) imaging is used widely in clinical practice across the world to assess fetal growth and abnormalities. 2D quantification and measurements of different structures (e.g., fetal head circumference, femur length, etc.) are widely used. However, 3D quantification and volumetric measurements of structures have unique challenges. Although US is a safe, inexpensive and real time imaging tool, the enhancement of US image quality is still limited. Furthermore, US acquisition has particular problems when imaging bony fetal structures because of the significant acoustic shadowing and signal drop out. Therefore, we hypothesize that post-processing 3D US images is important to improve quantification, measurement and diagnosis.

Previous clinical studies, for example [2-4], have quantified volumetric fetal structures such as the brain, femur, etc. Volumetric quantification of the semi-calcified fetal bone using US is inaccurate because of acoustic shadowing and hence part of the femoral volume may be missed [2]. The amount of missing bone depends on several factors including the degree of bone calcification, angle of acquisition and maternal tissue characteristics. In addition, the boundaries of the structures are often unclear. Therefore, volumetric quantification for such structures can be erroneous.

We propose a method to align and fuse multiple single view US images of the fetal femur acquired from different angles. Image fusion is the process of combining two or more aligned images. In other studies, 3D image fusion has provided good improvement in adult and fetal echocardiography. It has been used, for instance, to enhance boundary definition for adult heart chambers especially the left ventricle [1, 5-7]. A technique to align and fuse multiple 4D fetal echocardiography images to improve image quality was also presented in [8]. In addition, fusion can be used to extend the field of view by stitching multiple images with some overlap [1]. Our work is the first attempt in image fusion for 3D fetal bony structures in US. We have proposed a novel strategy for the fusion step which is validated on a fetal phantom and real data.

## 2 Method

### 2.1. Datasets

8 women with healthy pregnancies in the 2<sup>nd</sup> and 3<sup>rd</sup> trimester (20 to 30 weeks of gestation) participated in the study and gave their informed consent. In each case, 6 scans of the femur were taken from different angles of the longitudinal view. Scans were acquired using the same US machine (Philips HD9, Philips Healthcare, Bothell, Washington, USA). Scans for the same femur were taken in a consistent protocol. In each case, 6 scans were acquired such that the US beam was

approximately perpendicular to the mid shaft (2 scans), perpendicular to the distal epiphysis (2 scans) and perpendicular to the proximal epiphysis (2 scans). The first scan was the reference scan to which the remaining scans were aligned. The femur was imaged in a straight position for the first scan as shown in Figure 2 (a) and in any orientation for the remaining scans. Unfortunately, not all 6 scans could be used in the 8 cases because of misalignment of some images in the registration step. 2-5 scans were successfully aligned in each case. Scan dimensions were roughly  $120 \times 230 \times 120$  voxels. We have also used a fetal phantom (CIRS Model 068 Fetal Ultrasound Biometrics Phantom, CIRS, Norfolk, Virginia, USA). The simulated gestational age of the phantom is based on 21 weeks of gestation [7]. Ten scans for the fetal femur of the phantom were acquired from different angles.

## 2.2. Image Registration

During fetal scanning, the main transformations for the femur are translation and rotation since it is a rigid body. Therefore, we have adopted an automatic 3D rigid image registration algorithm to align fetal femur scans for the same fetus [1]. The optimization problem is formulated as follows

$$\arg \max_T S(T) = S(I_r, T(I_f^i)) \quad (1)$$

where  $S$  is the similarity measure,  $I_r$  is the reference image,  $I_f^i$  is the  $i^{\text{th}}$  floating image and  $T$  is the transformation function that is used to map  $I_f^i$  into  $I_r$  coordinate space.

We used the Normalized Cross Correlation (NCC) as a similarity measure as in [1]. We have also utilized a multi-resolution approach with multiple initializations to find the global maxima of the similarity measure. The Powell optimizer was used to maximize the similarity criteria. This process was performed between  $I_r$  (the first US image in every case) and  $I_f^i$  (the remaining US images in each case) and for every case. This process is time consuming but can be performed simultaneously.

It is always hard to judge the accuracy of a registration algorithm unless a ground truth deformation exists. We visually show registration results to show that the femur is correctly aligned and also other structures, e.g., thigh skin, knee tissues, etc, are correctly aligned. See green rectangles and the skin tissue in Figure 7 (a-c).

## 2.3. Wavelet-based Image Fusion

After image alignment in one coordinate space, image fusion can be performed in different ways [1]. US images contain a high amount of speckle and can have weak boundary definition. Therefore, we have developed a wavelet-based fusion that enhances the fetal femur US images. We have chosen to use the 3D Discrete Wavelet Transform (3D-DWT) in order to manipulate low and high frequency sub-bands. The process of the wavelet-based fusion is illustrated in Figure 1.

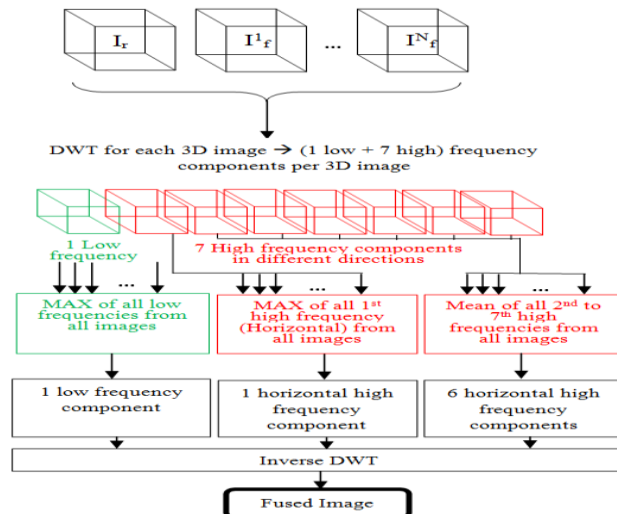


Figure 1. Framework of the wavelet-based image fusion.

The 3D-DWT is applied to every 3D US volume to get 8 frequency components from each volume. Figure 2 shows an example of wavelet decomposition. The low frequency component is a down-sampled intensity component of the original image. The remaining seven are the high frequency components in different orientations. The first high frequency component captures the horizontal intensity variations in the image. In this image, larger values are assigned to horizontal edges. In particular, this suggested to maximize the low and the horizontal high frequency components; e.g.,  $\text{MAX}(\text{low}_r, \text{low}_f^1, \dots, \text{low}_f^N)$  and  $\text{MAX}(\text{high}(1)_r, \text{high}(1)_f^1, \dots, \text{high}(1)_f^N)$  where  $r$  is the reference image and  $f$  is the  $i$ <sub>th</sub> floating image. On the other hand, we need to suppress other high frequency components because they are mainly speckle noise and/or other non-horizontal tissue artifacts. Therefore, we average the remaining 6 non-horizontal high frequencies.

After finding  $\text{MAX}_{\text{low}}$ ,  $\text{MAX}_{\text{high1}}$  and  $\text{AVG}_{\text{high2-7}}$ , we apply the inverse 3D-DWT to get the fused 3D image. See Figure 7 for a visual example.

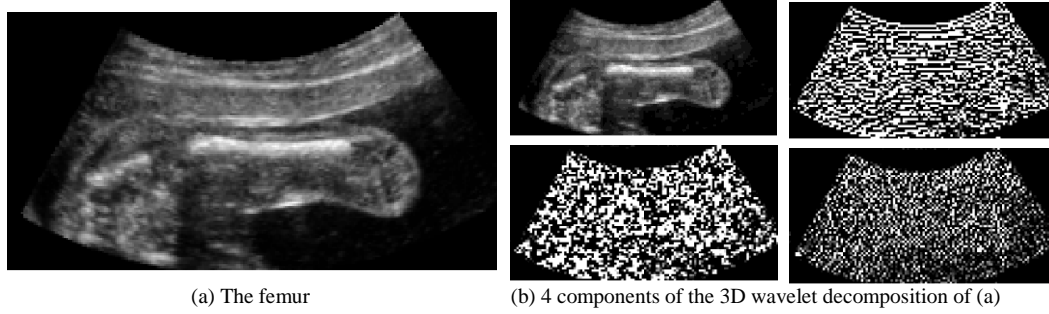


Figure 2. Example of 3D wavelet decomposition of the fetal femur. Only 2D slice (a) is shown with the 4 out of 8 3D wavelet decomposition components. (b) Top left is the low frequency (approximation), top right is the first high frequency component (horizontal details), bottom left is the second high frequency component and bottom right is the seventh high frequency component (vertical details). We binarize the high frequency components for visualization purpose.

## 2.4. Validation

We performed qualitative and quantitative validation. In the qualitative validation, an experienced clinician ranked all single view scans and fused views for all femurs. A score from 1 to 10 was given to each scan such that 10 means good femur definition and 1 means poor femur definition. The ranking took into account the contrast at the edge of the femur with a focus on the distal margins. Patient information was anonymized and images were randomly presented.

In the quantitative analysis, two intensity-based enhancement measures were estimated [1]. The measures are the percentage change of contrast and the percentage change of Signal to Noise Ratio (SNR), and they are defined as follows

$$\Delta \text{Contrast} = \left( \frac{\mu_{\text{fused}}^{\text{femur}} - \mu_{\text{fused}}^{\text{background}}}{\frac{1}{M} \sum_{i=1}^M \mu_i^{\text{femur}} - \mu_i^{\text{background}}} - 1 \right) * 100 \quad (2)$$

$$\Delta \text{SNR}^{\text{femur}} = \left( \frac{20 * \log \left( \frac{\mu_{\text{fused}}^{\text{femur}}}{\sigma_{\text{fused}}^{\text{femur}}} \right)}{\frac{1}{M} \sum_{i=1}^M 20 * \log \left( \frac{\mu_i^{\text{femur}}}{\sigma_i^{\text{femur}}} \right)} - 1 \right) * 100 \quad (3)$$

where  $\mu$  and  $\sigma$  are the mean and standard deviation within a region  $R$ , respectively;  $M$  is the number of images used in the fusion process (according to Figure 1,  $M=N+1$ ).  $R$  is a 2D representative region from the object of interest (the femur and background) of size  $10 \times 10$  pixels. The background region is selected from the thigh tissue directly above the femur. Since the region is 2D and can hardly capture the 3D structure, 20 different regions, 10 from the background and 10 from the femur were used in every image. The mean  $\Delta \text{Contrast}$  and  $\Delta \text{SNR}^{\text{femur}}$  were calculated for these regions.

For 2 of the real femurs, the single views and the fused image were manually segmented. The union and intersection of the segmented single views with the segmented fused femur were compared. In addition, a visual comparisons between our method and the Max, Mean methods [1] are shown in Figure 4. Notice that the wavelet-based method preserves more meaningful information than the other two techniques.

### 3 Results

#### 3.1. Qualitative Analysis

Figure 3 shows the scores from an experienced clinician. For all cases, the score for the fused view is 8 or higher and is always better than the maximum score given for any of the single view images except in one case where one of the single views has equal score with fused view (but also given a high score).

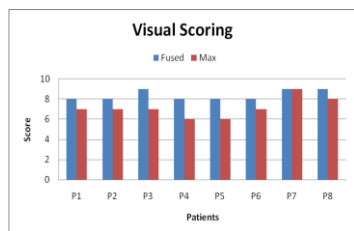


Figure 3. Scores from an experienced clinician. *Fused* is the score given to the fused images while *Max* is the maximum score given to any of the single view images used in fusion.

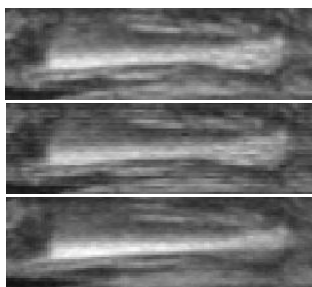


Figure 4. Visual comparisons between different fusion methods. Top: wavelet-based. Middle: Max. Bottom: Mean [1].

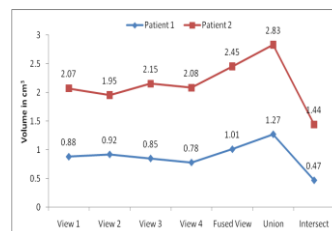


Figure 5. Comparing the femur volumes on four single views, fused view, union and intersection of the single views.

#### 3.2. Quantitative Analysis

The percentage change of contrast and the percentage change of SNR are shown in Table 1. Better contrast and SNR means that the percentage change should be positive, which is the case in all datasets. Fusion has enhanced the contrast and SNR by about  $16 \pm 18\%$  and  $8 \pm 4\%$  respectively. We also show the effect of fusion on the femur of the fetal phantom (Figure 6). Although the contrast of the whole image (the femur and its surrounding tissues) has increased, one can clearly see that the fused view has better boundary definition of the femur.

Two datasets (21 and 29 weeks gestation) were manually segmented. Each one has four single views. The percentage intersection with the fused view for the 4 aligned single views was 47% and 59% respectively. Although the four single views were aligned, each one highlights a different part of the femur. This clearly shows how the fused image provides better femur anatomical definition. For both patients the fused view has about 15% more volume than the mean volume of the 4 single views. On the other hand, the volume of union between the four single views is larger than the volume of the fused view for both datasets. The union volume was respectively 26% and 16% larger than the fused volume. This is mainly because of the unclear boundaries of the distal and proximal epiphysis which in turn lead to an inaccurate manual segmentation. Figure 7 (d-f) shows manual segmentation results and Figure 5 shows volume comparisons for both cases.

The registration on average takes three to four minutes to register two 3D volumes. On the other hand, fusion requires around five seconds to fusing four aligned images. The code runs on a 2.8 GHz quad core PC with 8GB of RAM. The registration time is high but this is because it is a multi-resolution, multi-initialization algorithm. In general, registration between the views is independent and can be performed simultaneously.

### 4 Discussion and Conclusions

In this paper we describe the development of an automatic technique to register and fuse multiple 3D US images of the fetal femur. We present a novel processing in the wavelet domain to improve the femur boundary definition. Interestingly, we showed that the intersected femur volume between four aligned single view 3D US images is roughly 50% of the fused femur volume. In addition, the fused femur volume is about 15% more than the mean of 4 single views. This implies that 3D quantification from single views may be inaccurate. Future work will evaluate how the extra level of anatomical definition provided by 3D fusion can be used to quantify fetal bone development and the effect of fusion on automatic fetal femur segmentation [9].

Table 1. Percentage improvement of Contrast & SNR between single views and fused images.

	% Contrast	% SNR
Patient 1	16	11
Patient 2	55	13
Patient 3	9	10
Patient 4	5	4
Patient 5	5	1
Patient 6	15	8
Patient 7	5	4
Patient 8	19	3
Phantom	6	13

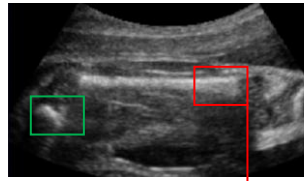


(a) Single view

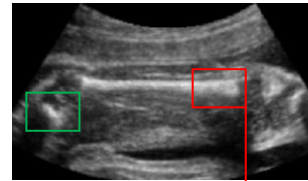


(b) Fused view

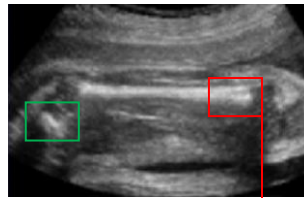
Figure 6. The femur of a fetal phantom. (a) 2D slice of one single view out of 10 is shown with (b) the corresponding 2D fused slice.



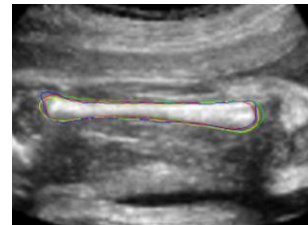
(a) Aligned single view 1



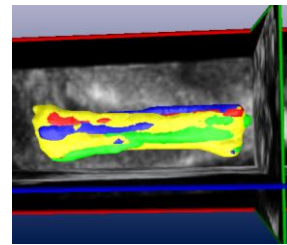
(b) Aligned single view 2



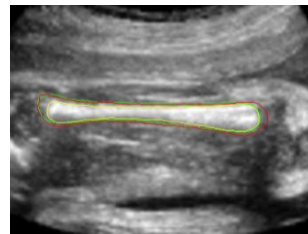
(c) Fused view



(d) Segmentation from four single views over the fused image



(e) 3D Surface: 4 single views segmentation over the fused image



(f) The segmentation on the fused image. Fused (green), union (red) and intersection (yellow)

Figure 7. Detailed comparisons using the manual segmentation on aligned and fused view. The green rectangle shows the correct alignment of another structure (partial tibia bone).

## References

- [1] K. Rajpoot, "Multi-view 3D Echocardiographic Image Analysis," Department of Engineering Science, University of Oxford, Oxford, 2009, PhD Thesis.
- [2] P. A. Mahon *et al.*, "The use of 3D ultrasound to investigate fetal bone development," *Norsk Epidemiologi*, vol. 19(1), 2009.
- [3] C.-H. Chang *et al.*, "Prenatal Detection of Fetal Growth Restriction by Fetal Femur Volume: Efficacy Assessment Using Three-Dimensional Ultrasound" *UMB*, vol. 33(3), pp. 335-341, 2007.
- [4] C.-H. Chang *et al.*, "The assessment of normal fetal brain volume by 3-D ultrasound," *UMB*, vol. 29(9), pp. 1267-1272, 2003.
- [5] K. Rajpoot *et al.*, "Multiview RT3D Echocardiography Image Fusion," in *FIMH 2009*, 2009, pp. 134-143.
- [6] P. Soler *et al.*, "Comparison of Fusion Techniques for 3D+T Echocardiography Acquisitions from Different Acoustic Windows," in *Computers in Cardiology*, 2005.
- [7] C. Smigielski *et al.*, "Four-Dimensional Fusion Echocardiography: A New Technique for Fusion of Real-Time Three-Dimensional Datasets Obtained from Different Transducer Positions: First Clinical Experience," *in press JACC: CVI* 2010.
- [8] M. J. Gooding *et al.*, "Investigation into the fusion of multiple 4D fetal echocardiography images to improve image quality," *in press UMB*, 2010.
- [9] MAVIDOS. "http://www.wren.soton.ac.uk/pdf/MAVIDOS Abstract format for newsletter Jan08.pdf," 24/3/2010.